Materials Research, Vol. 11, No. 2, 199-205, 2008

Microstructural Development and Tensile Strength of an ECAP - Deformed Al-4 wt. (%) Cu Alloy

*Érika Ferananda Prados, Vitor Luiz Sordi, Maurizio Ferrante**

Department of Materials Engineering, Federal University of São Carlos – UFSCar, São Carlos - SP, Brazil

Received: March 3, 2008; Revised May 20, 2008

The tensile strength of metals and alloys can be considerably increased by severe plastic deformation, a consequence of the extreme grain refinement thus achieved. In the present work the deformation was performed by Equal Channel Angular Pressing and the material was an Al-4% Cu alloy. Characterization included tensile tests, and microstructural observation by optical and transmission electron microscopy. After four passes, the yield strength showed an increase of 310% over the undeformed alloy, a figure reduced to 160% by a 250 °C / 1 hour post - deformation anneal. Additionally, the alloy displayed a very low work hardening capacity, especially after the annealing heat treatment. After four deformation passes the grain size of the annealed specimens was estimated to be close to 500 nm. The tensile behaviour and the absence of work hardening were discussed in terms of the fine microstructure.

Keywords: *ECAP, Al-4%Cu, SPD, tensile properties, microstructure, work-hardening*

1. Introduction

In the last ten years a large number of investigations regarding a severe plastic deformation (SPD) technique called Equal Channel Angular Pressing (ECAP), were published in the wake of the pioneering work by Valiev et al.[1] and Segal[2]. Justification for this interest lies in the fact that ECAP- deformed metals and alloys exhibit a very small grain size and consequently, their tensile strength is remarkably improved. All relevant work on this SPD technique has been recently summarized by Valiev and Langdon in a comprehensive review[3]. The microstructural evolution of metals and alloys subjected to low and medium plastic deformation has been discussed by Liu and Hansen[4], and Bay et al.[5]. The outcome of these studies is a model describing how, in severely deformed metals with high to moderate stacking fault energy, grain subdivision takes place by the formation of cell blocks separated by arrays of geometrically necessary dislocations. Within these cells there are regions relatively free from dislocations, bounded by low angle boundaries. The more severe the deformation, the narrow the cell blocks become, until the cell boundaries transform into high angle boundaries. This sequence has been often observed in ECAP - deformed metals and alloys and seems to explain the formation of very small grains[6,7]. A still active dispute is how the high angle dislocation boundaries transform into grain boundaries; on this respect, a study by Chang et al.[8] identified three types of boundaries in commercially pure Al subjected to ECA - deformation: i) polygonized dislocation walls of the type described by Bay et al.[5]; ii) partially transformed boundaries, and iii) proper grain boundaries. The evolution of type i to type iii takes place by the dissociation of lattice dislocations and their absorption into the boundaries. This process decreases the free energy of the system since the resulting grain boundaries are of the equilibrium type.

As for the tensile behaviour, strength enhancement is a consequence of the very small grain size, and as such the Hall-Petch relationship still applies, since for ECAP- deformed materials the grain size does not go below ≈ 200 nm and said relationship only breaks down for grains smaller than ≈ 25 nm[9]. Of course, in SDP materials, dislocation hardening must contribute to the total strength, but the relative proportion is unknown; at any rate, grain size hardening is the dominant mechanism. Although ductility loss appears to be a customary occurrence, improvement of that property was observed in some cases and attributed to the non-equilibrium state of the grain boundaries, which allows mechanisms such as boundary sliding and grain rotation[10]. However, direct evidence of these mechanisms is still lacking.

This work reports on a number of observations performed on an Al-4wt%Cu alloy containing a coarse dispersion of Al_2Cu particles. Deformation was carried out by ECAP in a $\Phi = 120°$ die. Tensile behaviour and microstructural evolution were characterized and discussed, keeping in view the current theories on both substructure formation and the enhancement of tensile properties by SPD.

2. Experimental

2.1. Material

An Al-Cu alloy was prepared in an induction furnace by melting commercially pure Al and electrolytic Cu. Chemical composition was Al-4.1% Cu-0.067% Fe and the alloy was poured into a steel mould from which prismatic samples with dimensions 14 x 14 x 75 mm^3 were machined out and subsequently homogenized at 530 °C / 24 hours. This was followed by furnace cooling so as to obtain large Al_2Cu precipitates.

2.2. ECA deformation

A die with $\Phi = 120°$ and $\psi = 0°$ (inner and outer radii of curvature equal to 8 mm) was employed. The control sample was identified as 0X and the deformed samples as 1X, 2X, … etc. with the numeral indicating the number of passes. Pressing was carried out in a 25 t INSTRON model 5500R operating at 5 mm per minute. Route A was employed, meaning that the sample is pressed without rotation between passes, the lubricant was a Mo_2S paste and a maximum of five passes was applied. Figure 1 shows the die, its geometrical

*e-mail: ferrante@power.ufscar.br

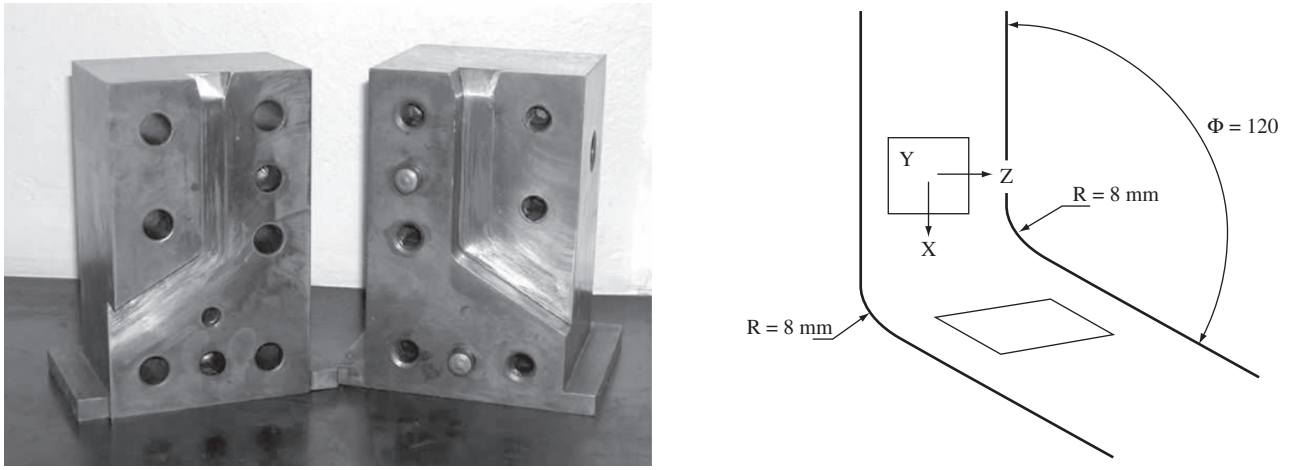

Figure 1. Photograph of the ECAP die and schematic of the geometry of the die channel, plus sample planes identification.

parameters, the X, Y and Z planes of the sample and their orientation with respect to the die.

2.3. Post-deformation heat treatment

The deformed samples were annealed at 250 °C / 1 hour, thus forming the XR series of samples: 0XR, 1XR, 2XR… etc. Some samples were annealed at 300 °C / 1 hour.

2.4. Characterization

Tensile tests were employed to determine maximum tensile stress, yield stress, elongation, strain hardening exponent and deformation energy to fracture, also known as static toughness. Calculation of the strain hardening exponent followed the procedure given by ASTM E 646 – 00† whilst static toughness was given by the total area under the engineering stress - strain curve. Flat tensile specimens were machined out from the ECAP deformed samples by spark erosion; dimensions were 3 x 2 mm^2 and 13 mm gauge length. Transmission electron microscopy (TEM) was employed to follow the microstructural development of the deformed and post - deformed annealed samples, as a function of pass number. Thin foils observation was carried out in a Phillips® CM 120 electron microscope; specimens were prepared by polishing 3 mm diameter discs until perforation in a TENUPOL3 equipment and the electrolytic solution consisted of methanol / nitric acid in the proportion of 7 to 3. Operating conditions were 15-20 V and –30 °C. Conventional light microscopy completed the microstructural characterization.

3. Results

3.1. Tensile properties

Figure 2a shows the engineering stress strain curves of undeformed and ECAP - deformed specimens, the latter group tested in the as-deformed condition and after annealing. It can be seen that both strength and elongation increase with the number of passes; the graph in Figure 2b gives a more precise description of the tensile behaviour, which can be summarized as follows: i) maximum strength is attained after four passes; ii) elongation increases with respect to the undeformed sample, but there is a sharp ductility drop after the first pass; however, elongation gradually recovers reaching a maximum after pass number four; iii) yield strength and ductility increase slowly up to 310% and 33% with respect to the undeformed sample; and iv) annealing at 250 °C causes a ≈ 20% decrease of yield strength (for 4XR), combined with a substantial ductility improvement (+ 63%) over the 4X specimen. Finally, the work-hardening effect was very low, particularly for the annealed samples.

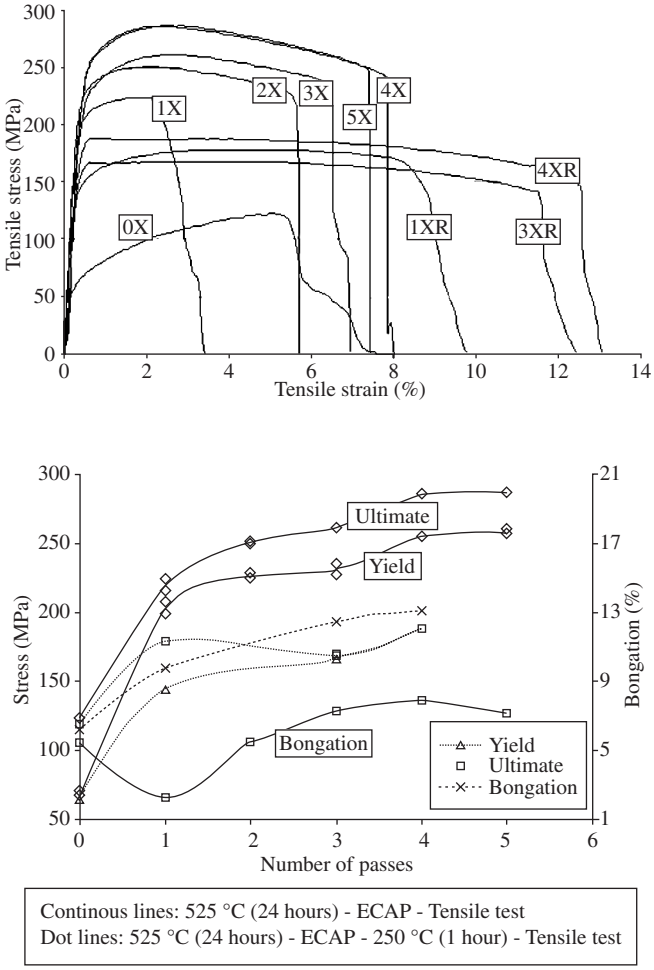

Figure 2. Tensile data of the Al-4% Cu alloy in the undeformed, ECA - deformed and post-deformation annealed conditions: a) engineering stress-strain curves; b) test parameters, that is, yield, ultimate strength and elongation.

† Standard Test Method for Tensile Strain-Hardening Exponents (n-Values) of Metallic Sheet Materials: plastic true strain and true stress were fitted to the Hollomon expression $\sigma = k\,\varepsilon^n$.

More detail on the work hardening behaviour is given in Figure 3, where the parameters of the Hollomon equation, $\sigma = k\,\varepsilon^n$, are plotted as a function of the number of passes. These results show that the exponent **n** decreases continuously with deformation up to approximately one fifth of the original value (0X sample), whilst k scales with the maximum strength.

Finally, the static toughness was calculated as a function of the imposed shear strain, calculated by the Iwahashi formula[11]. Figure 4 shows the data and includes results obtained by Fang and co-workers on an Al-3.9% Cu alloy[12]; it can be seen that the deformation energy values obtained in the present investigation are consistently higher.

3.2. Microstructure

Figure 5 shows optical micrographs illustrating the microstructural evolution of the Al-4% Cu alloy with ECAP - deformation. Main features are: i) severe grain elongation, and macroscopic shear patterns with angular ranges slightly different from those theoretically predicted by Furukawa, Horita and Langdon[13], see Figures 5a,b,e; ii) fracture of the large precipitates formed during slow cooling, a phenomenon better imaged in Figure 5c; and iii) internal fragmentation of the elongated grains, making an angle of approximately 60° with the pressing direction see Figure 5d.

The fine microstructure is revealed by TEM, see examples in Figure 6. The corresponding diffraction patterns show that the 1X specimen contains a high proportion of low angle boundaries, see streaked diffraction spots, whilst further deformation increases grain misorientation, as revealed by the ringed diffraction pattern produced by the 4X sample.

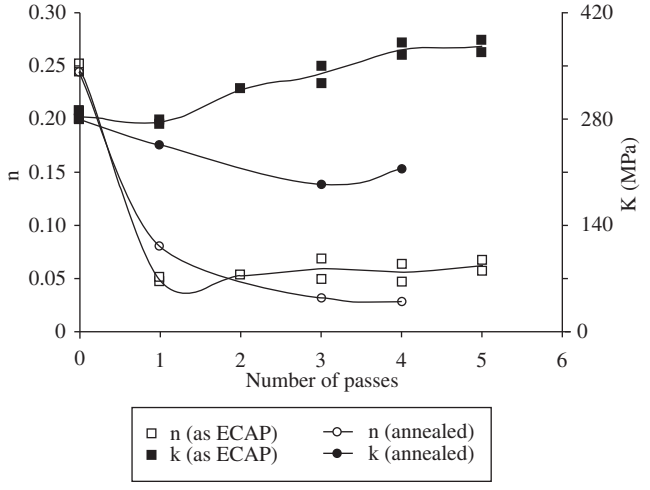

Figure 3. Evolution of the parameters of the Hollomon equation with the number of ECAP passes.

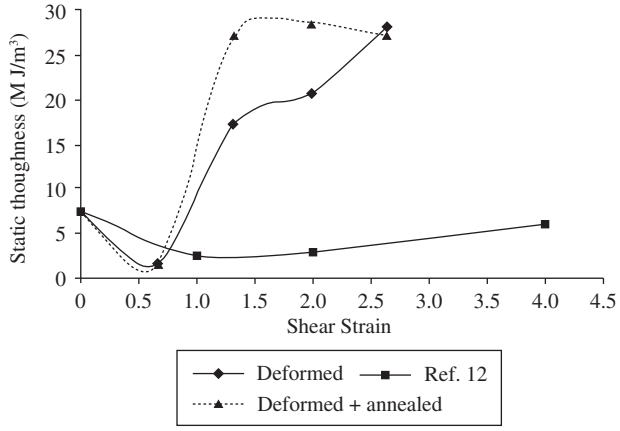

Figure 4. Evolution of the static toughness as a function of shear strain.

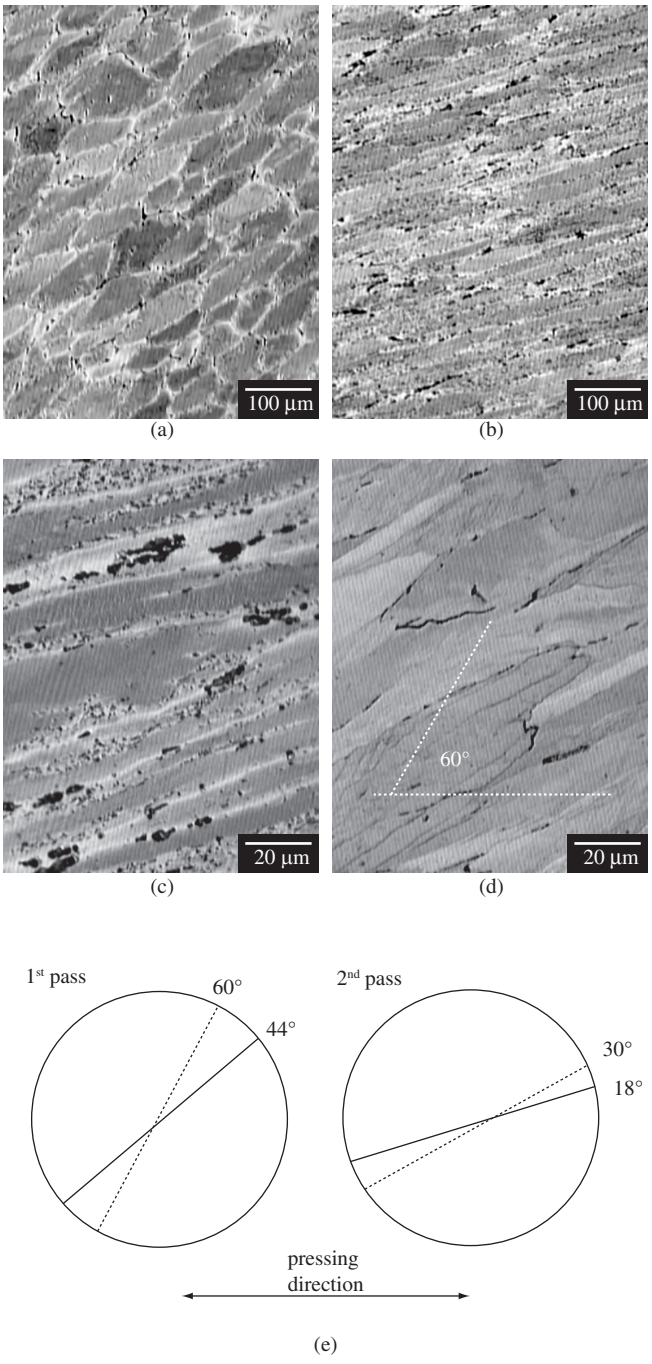

Figure 5. Optical micrographs of the ECAP-pressed samples taken on plane Y: a) after one pass; b) after two passes; c) higher magnification of the 2X sample, showing alignment and fracturing of the Al_2Cu particles; d) example of grain internal fragmentation in a 2X specimen; e) theoretical (dotted lines) and observed (solid lines) angular ranges of the slip traces on plane Y.

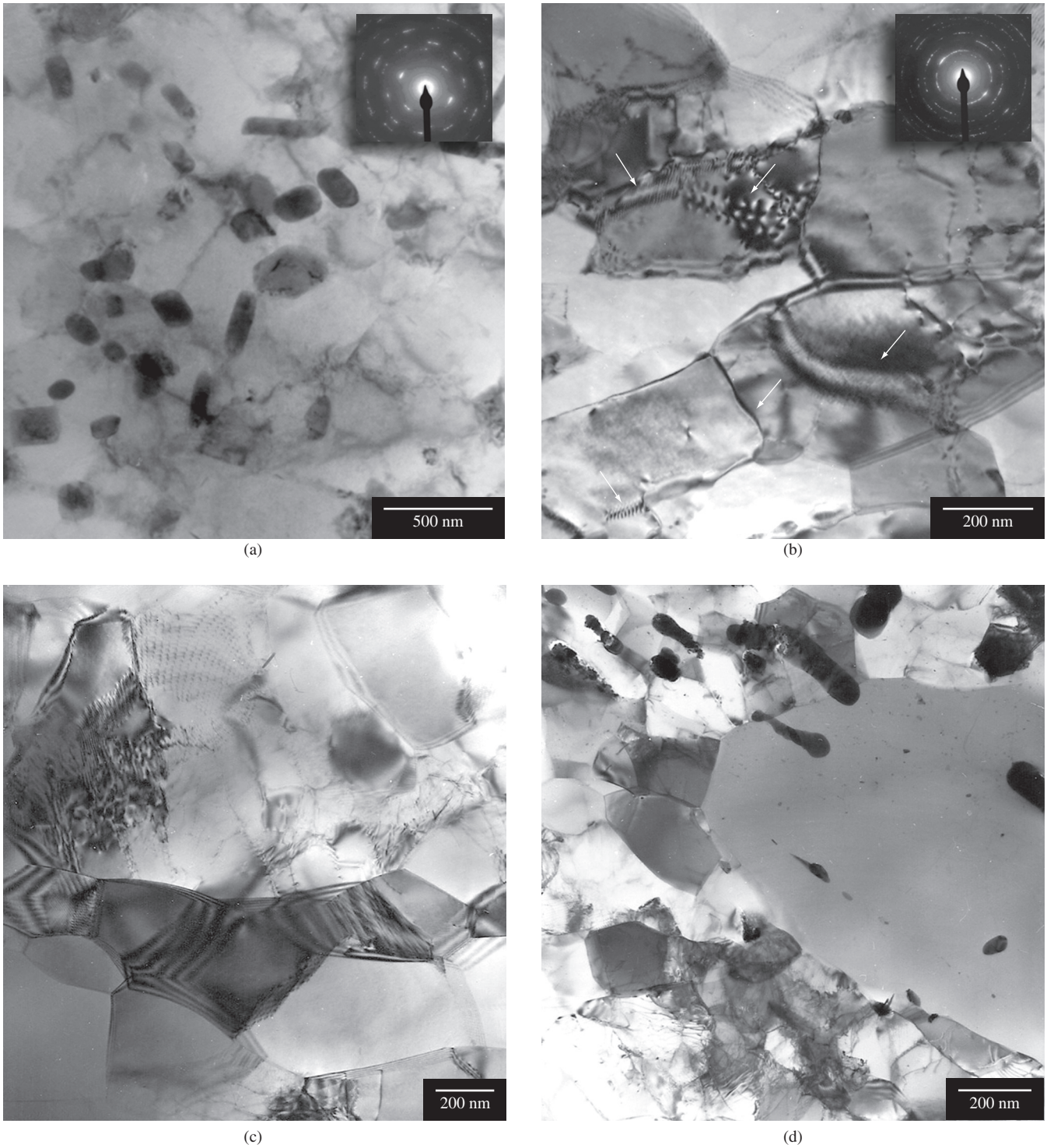

(a) (b) (c) (d)

Figure 6. TEM micrographs of deformed samples: a) 1X specimen; b) 4X specimen; c and d) samples 4XR, annealed at 250 °C and 300 °C, respectively.

4. Discussion

Although most investigations employed dies with channels making 90°, a different solution, that is, $\Phi = 120^{o}$, was quite satisfactory despite a lower strain per pass, see Iwahashi formula[11]. Indeed, the association of this angle with Route A, which is the practice employed in the present set of experiments, was identified as the optimal procedure for Al alloys[14,15].

4.1. Tensile properties

The considerable increase of tensile strength shown in Figure 2 is a characteristic of severely deformed metals and alloys. However, in most reported cases the ductility decreases, but surprisingly the present results show the opposite trend. To understand this result it must be pointed out that the ductility of the reference sample (0X) was relatively low. From this, plus detailed observation of the fracture

morphology of the tensile specimens, a different picture emerges. Indeed, from Figure 2, it can be seen that the elongation of the reference sample is equal to 6.2%, a very low figure; in comparison, a separate experiment in which an identical alloy was conventionally extruded and tested in tension showed elongation equal to 19%. Figure 7 is a scanning electron micrograph of the 0X sample fracture surface[16]; solidification voids are clearly seen, and a void-dominated fracture path is consistent with the wavy stress - strain curve of this sample, see Figure 2, which also shows that fracture takes place with no area reduction. In conclusion, the ductility improvement here observed is an artifact due to the low initial ductility of the cast alloy. However, the solidification defects seems to have been progressively healed by the ensuing passes and this is consistent with the observed ductility enhancement observed from the second pass on.

Another important feature of the tensile behaviour here observed is the absence of work hardening. This is a common occurrence in ECA-deformed material, consistently attributed to the low density of mobile dislocations due to mutual annihilation and absorption by the grain boundaries. These mechanisms are made easy in nano and sub-microcrystalline materials by the small diffusion distances[17], or by dynamic recovery[18]. The latter phenomenon is likely to occur in Al since room temperature corresponds to approximately 0.3 T_m (homologous temperature). A practical consequence of the lack of work hardening is unstable deformation leading to fast necking and specimen fracture. However, Figure 2 shows that a very large fraction of the total elongation takes place after the onset of necking, in other words, from the point of maximum stress, up to the fracture strain. For instance, taking the 4X sample, it can be seen that more than 70% of the total deformation occurs in the non-homogeneous deformation regime, in other words, necking is a very slow process. Furthermore, after the annealing heat treatment that regime occupies almost the total strain undergone by the sample. This behavior is an indication of superplasticity, which is one among the benefits of the ECAP technique[19], but of course, its full achievement requires a combination of strain rates and testing temperatures which are outside the scope of the present paper. Finally, Figure 3 clearly indicates that the work hardening capacity is further decreased by the 250 °C post - deformation heat treatment. The explanation resides in the difference of intragranular dislocation density, which is lower in the annealed samples, and in other fine microstructure features, such as grain (or sub-grain) size and the nature of the internal boundaries.

As for the influence of the deformation level on work hardening, more information is gathered from Figure 8, an enlargement of the engineering stress - strain curves of the annealed ECAP samples. It is apparent that the extent of work hardening of the 1XR and 4XR samples is different, and possible causes are differences on the dislocation density and their annihilation rate. These tentative statements will be justified when discussing the fine microstructure.

4.2. Microstructure

The optical micrographs show grain elongation and slip traces making an angle of 45° (first pass) with respect to the extrusion direction and 18° (second pass), see Figures 5a,b,e. However, the corresponding theoretical shear angles are 60° and 30°, see dotted lines in Figure 5e. The discrepancy between the theoretical[13] and experimental macroscopic shear angles can be explained by the fact that the former were calculated assuming inner and outer curvature radii equal to zero, while the ECAP die here used was designed with R = r = 8 mm. Consequently shear does not take place along a single plane, but along a fan - like sheaf of planes. Finally, Figure 5d shows that the direction of grain fragmentation makes 60° with the pressing direction; this fragmentation is a general occurrence, which presumably takes place along the most active slip systems, that is, [111] and

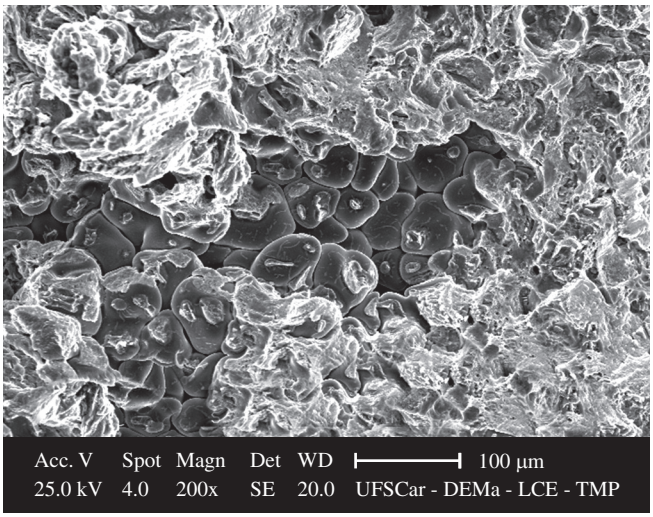

Figure 7. Scanning electron microscope fractography of the 0X (non deformed) tensile specime fracture surface showing a large shrinkage void.

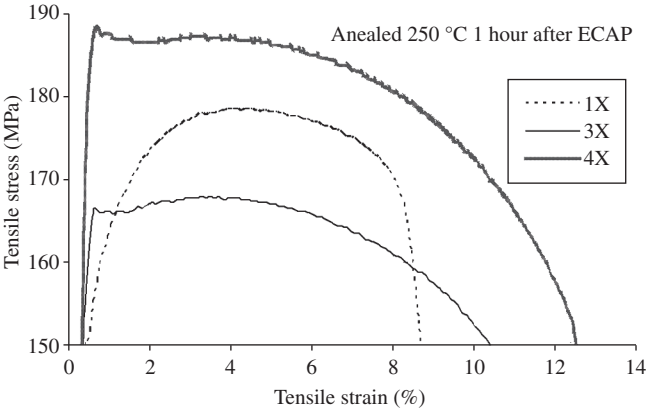

Figure 8. Engineering strain - stress curves of three post-deformation annealed specimens (enlargement of fig 2-a).

<110>. Said feature is related to the macroscopic grain orientation and in a previous paper[20] a numerical description of the evolution of the grain axes orientation was developed, with results displaying a relatively good match with TEM observations by Wu et al.[21]. As for the fine microstructure, Figure 6 shows that the diffraction pattern of the 1X sample exhibits incomplete rings indicating low angle boundaries or, more precisely, sub-boundaries, whilst in the 4X sample the ring pattern is more continuous, meaning that the sub-boundaries have turned into high angle boundaries. In the introduction it has been mentioned that such evolution from low to high boundaries is supposed to be the main mechanism responsible for crystalline grain formation. The large particles shown in Figure 6a are Al_2Cu precipitated during the slow cooling from the homogenizing temperature. In the 4X sample, non-equilibrium boundaries, probably formed by polygonized dislocation walls[7] are indicated by the arrows; the non-equilibrium condition is also revealed by the strong diffraction contrast near the boundaries, an indication of elastic strain.

After annealing the deformed samples exhibit different microstructures, see Figure 6c,d showing the 4XR specimen annealed at 250 °C and 300 °C, respectively. In the former micrograph the main characteristics are the formation of equilibrium or near - equilibrium

boundaries and a lower dislocation density. The nature of the grain boundaries is indicated by the presence of well defined extinction contours which, according to the dynamic theory of diffraction contrast are contours of similar grain depth in a thin foil; they appear in TEM images when some family of planes of the given grain is in the Bragg reflection condition. Additionally, the grains show straight sides, which is another characteristic of equilibrium boundaries. As for the 300 °C annealed material, see Figure 6d, the following features are relevant: i) accentuated coarsening of the Al_2Cu precipitates; ii) the grain interiors appear to be totally free from dislocations; iii) complete recrystallization, and iv) discontinuous grain growth. That the 300 °C anneal is sufficient to fully recrystallize the Al-4% Cu alloy is clearly shown by the hardness curve of Figure 9, obtained on a 4X sample, where softening begins at 250 °C and reaches the maximum value at 300 °C / 1 hour.

Figure 10 shows micrographs of the 1XR and 4XR samples, which are characterized by a very different work hardening behaviour, see Figure 8; examination of the fine microstructure suggests that both grain size and nature of the grain or sub - grain boundaries play an important role in that phenomenon. Indeed, from measurements performed on a number of TEM micrographs, of which Figure 10 is a typical example, the grain size of the 1XR and 4XR samples was found to be close to 700 and 400 nm, respectively. This means that dislocation absorption at the boundaries is easier in the latter since the defects mean free path is smaller, thus decreasing the likelihood of dislocation interaction. The second cause of lack of work hardening may be found in the grain boundary character, and from the diffraction patterns displayed in Figure 10, it is apparent that the proportion of high angle boundary is higher in the 4XR than in the 1XR sample. Recalling that the work hardening exponents of the aforementioned samples are 0.03 and 0.08, respectively, it can be concluded that the dislocation absorption rate depends also of the grain boundary character, being faster for high angle boundaries. Although it was not possible to separate the effect of grain boundary character from that of grain size, the results confirm data from Sun and collaborators who studied two groups of commercially pure Al samples of similar grain size but differing in the proportion of high angle boundaries, and found that work hardening was much lower when these boundaries are predominant[22]. On the other hand, a more recent paper on two groups of severely deformed Cu, exhibiting low and high angle boundaries showed the opposite trend[23]. However, the authors did not take into consideration that the groups also differed in grain size and dislocation density, having been produced by two different SPD techniques.

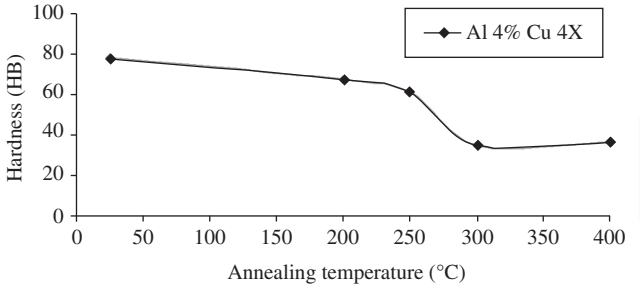

Figure 9. Hardness of sample 4x after annealing at 200, 250, 300 and 400 degrees Celsius.

Returning to the strain hardening differences shown in Figure 8, it is possible to further speculate on their causes by recalling that after one ECAP pass, the sub-boundaries are ill-defined, have low capacity for dislocation storage and continue to be so after the anneal. Hence, the "effective" grains are still large and the material exhibits the conventional work hardening behaviour. Indeed, Figure 8 shows that the 1XR sample strength is due to that phenomenon. Instead, the stress - strain curves of the other two samples are completely flat and their strength can be attributed to the small grain size.

At any rate, the influence of grain boundary character on the mechanism of strain hardening is still not fully understood.

5. Conclusions

After only four ECAP passes, the tensile strength of an Al-4%Cu alloy showed an increase of 300%, not too distant from the 250% displayed by sample 2X, meaning that grain size reduction is a fast process. Apparently, the elongation also increases but observation of the tensile specimens fracture surface suggests that the reference material, that is, the 0X sample had low ductility due to solidification defects. At any rate, the good combination strength - ductility resulted in very high values of static toughness, viz. 22 MJ m^{-2} displayed after four passes. Absence of work hardening was attributed

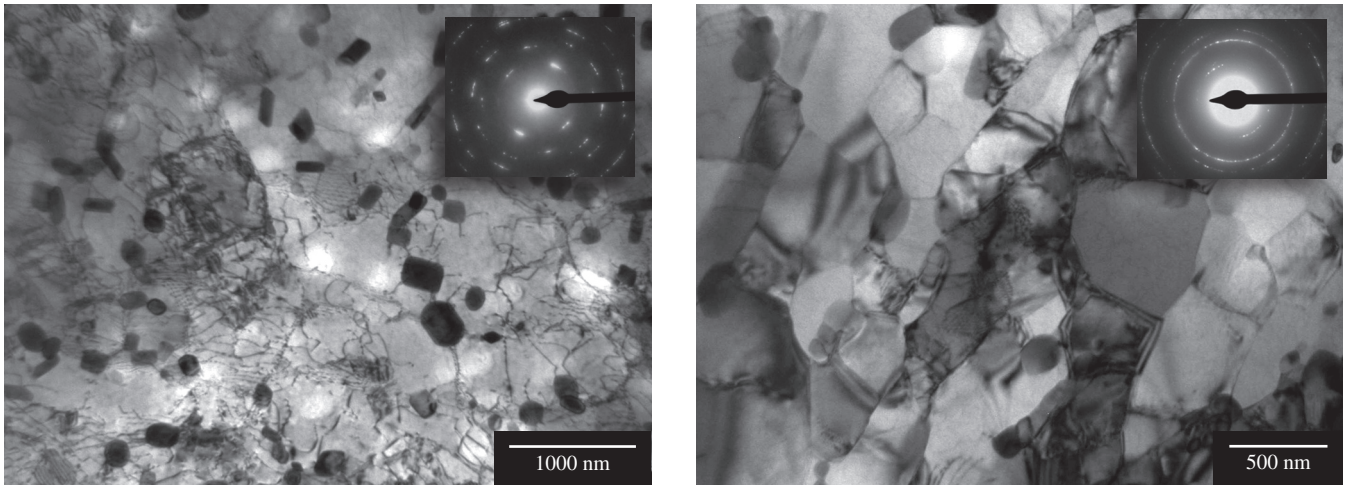

(a) (b)

Figure 10. Transmission electron microscope and diffraction patterns of samples 1XR and 4XR.

to the small distance between grain or sub-grain boundaries and to the grain boundary character: the larger the grain boundary angle the easier the dislocations are absorbed, thus, the working hardening phenomenon is reduced.

In conclusion, the present work shows that deformation by ECAP is a very efficient method to achieve high strength and reasonable ductility and that evaluation of the latter property needs a complete characterization of the raw material to avoid false comparisons. Also, it was ascertained that after the second pass, ECAP deformation exerts a defect closure effect, thus "correcting" unsound raw material. Finally, the work hardening behavior has been described and a tentative discussion on the relevant causes has been attempted

References

1. Valiev RZ, Korznikov AV, Mulykov RR. Structure and properties of ultrafine-grained materials produced by severe plastic deformation. *Materials Science Engineering A* 1993; 168:141-148.
2. Segal VM. Materials processing by simple shear. *Materials Science Engineering* A 1995; 197:157-164.
3. Valiev RZ, Langdon TG. Principles of equal-channel angular pressing as a processing tool for grain refinement. *Progress in Materials Science* 2006; 51:881-981.
4. Liu Q, Hansen N. Macroscopic and microscopic subdivision of a cold - rolled single crystal of cubic orientation. *Proceedings of the Royal Society* 1998; A454:2555-2591.
5. Bay B, Hansen N, Huges DA, Kuhlmann-Wilsdorf D. Overview no. 96 evolution of f.c.c. deformation structures in polyslip. *Acta Metallurgica Materialia* 1992; 40:205-219.
6. Xu C, Furukawa M, Horita Z, Langdon TG. Developing a model for grain refinement in equal-channel angular pressing. *Materials Science Forum* 2006; 503-504:19-24.
7. Iwahashi Y, Horita Z, Nemoto M, Langdon TG. The process of grain refinement in equal-channel angular pressing. *Acta Materialia* 1998; 46:3317-3331.
8. Chang CP, Sun PL, Kao PW. Deformation induced grain boundaries in commercially pure aluminium. *Acta Materialia* 2000; 48:3377-3385.
9. Meyer M, Mishra A, Benson DJ. Mechanical properties of nanocrystalline materials. *Progress in Materials Science* 2006; 51:427-556.
10. Valiev RZ, Alexandrov IV, Zhu YT, Lowe TC. Paradox of strength and ductility in metals processed by severe plastic deformation. *Journal of Materials Research* 2002; 17:5-8.
11. Iwahashi Y, Wang J, Horita Z, Nemoto M, Langdon TG. Principle of equal-channel angular pressing for the processing of ultra-fine grained materials. *Scripta Materialia* 1996; 35:143-146.
12. Fang DR, Zhang ZF, Wu SD, Huang CX, Zhang H, Zhao NQ, Li JJ. Effect of equal channel angular pressing on tensile properties and fracture modes of casting Al-Cu alloys. *Materials Science Engineering* 2006; A426:305-313.
13. Furukawa M, Horita Z, Langdon TG. Factors influencing the shearing patterns in equal-channel angular pressing. *Materials Science Engineering* 2002; A332:97-109.
14. Gholinia A, Prangnell PB, Markushev MV. The effect of strain path on the development of deformation structures in severely deformed aluminium alloys processed by ECAE. *Acta Materialia* 2001; 48:1115-1130.
15. Zhu YT, Lowe TC. Observations and issues on mechanisms of grain refinement during ECAP process. *Materials Science and Engineering* 2000; A291:46-53.
16. Prados E, Sordi V, Ferrante M. (artigo a ser publicado). *Materials Science Engineering (2008).*
17. Park JH, Lee YS, Nam WJ, Park KT. Comparison of compressive deformation of ultra - fine grained 5083 Al alloy at 77 and 298 K. *Metallurgical Transaction A* 2005; 36A:1365-1368.
18. Wang YM, Ma E. Strain hardening, strain rate sensitivity, and ductility of nanostructured metals. *Materials Science Engineering A* 2004; 375-377:46-52.
19. McFadden SX, Mishra RS, Valiev RZ, Zhilaev AP, Mukherjee AK. Low-temperature superplasticity in nanostructured nickel and metal alloys. *Nature* 1999; 398:684-686.
20. Signorelli JW, Turner PA, Sordi V, Ferrante M, Vieira EM, Bolmaro RE. Computational modeling of texture and microstructure evolution in Al alloys deformed by ECAE. *Scripta Materialia* 2006; 55:1099-1102.
21. Wu PC, Chang CP, Kao PW. The distribution of dislocation walls in the early processing stage of equal channel angular extrusion. *Materials Science Engineering A* 2004; 374:196-203.
22. Sun PL, Cerreta EK, Bingert JF, Gray(III) GT, Hundley MF. Enhanced tensile ductility through boundary structure engineering in ultrafine-grained aluminum. *Materials Science Engineering A* 2007; 464:343-350.
23. Zhao YH, Bingert JF, Zhu YT, Liao XZ, Valiev RZ, Horita Z, Langdon TG, Zhou YZ, Lavernia EJ. Tougher ultrafine grain Cu via high-angle grain boundaries and low dislocation density. *Applied Physics Letters* 2008; 92:081903-05.